Okhotsk Sea and Polar Oceans Research 5 (2021) 1-6

https://doi.org/10.57287/ospor.5.1

Review

Arctic warming amplification and warming suppression in East Antarctica - Contribution of MOC to north-south asymmetry -

Takashi YAMANOUCHI [1, 2]

[1] *National Institute of Polar Research, Japan*
[2] *SOKENDAI (The Graduate University for Advanced Study), Japan*

(Received October 3, 2020; Revised manuscript accepted November 20, 2020)

Abstract

Warming amplification in the Arctic and warming suppression in the Antarctic are seen. What makes this great contrast under global warming? Several mechanisms to make this contrast have already been discussed; however, one of the most effective is ocean circulation, called meridional overturning circulation (MOC). Here, we will review the progress of studies in the recent decade of how MOC contributes to the large North-South asymmetry in warming.

Key words: Arctic amplification, Antarctic, warming suppression, asymmetry, meridional overturning circulation

1. Introduction

Under global warming, extreme warming occurs in the Arctic, more than twice the global average since 1970, and we call this increase as "Arctic amplification." Also, strong warming is seen in the Antarctic Peninsula, comparable to the Arctic. However, the surface air temperatures in East Antarctica show no clear warming trends, and we call this "warming suppression." This great contrast in the surface air temperature (SAT) trends between the Arctic and East Antarctica, even in the polar regions, is of great concern and the target of the present review.

Many ideas – theories – are introduced in the recent to explain this contrast or extreme phenomena in the one side of the polar region. The famous hypothesis in atmospheric science is the warming suppression by the ozone hole proposed by Thompson and Solomon (2002). Since the ozone hole seems to recover within a few decades (~ 2060), this hypothesis would be verified. Another idea is the difference in the surface topography between the Arctic and Antarctica. The high surface topography of the Antarctic ice sheet prevents the intrusion of air from the lower latitude. In comparison, the Arctic ocean's sea level allows the intrusion of warm-moist air from the lower latitude, which contributes to warm the Arctic (Yamanouchi, 2019). Also, the Antarctic ice sheet's high surface elevation makes the surface temperature much colder than the Arctic surface. It makes the outgoing longwave radiation (OLR) smaller in the Antarctic compared to the Arctic (Salzmann, 2017).

Another mechanism that derives the different warming trends is the difference in the area where the ice albedo feedback is effective (Goose and others., 2018). In the Arctic, ice albedo feedback works in most areas over the sea ice in the Arctic Ocean or over the land area where snow covers the surface in vast latitude regions. On the other hand, in the Antarctic, the area where ice albedo feedback is effective is limited to the sea ice area, which is restricted to 55 to 70° south, and not over the Antarctic ice sheet, where the surface snow cover could not change in the short time scale.

In addition to the many components responsible for the asymmetry of warming as introduced above, ocean circulation is another strong agent to make this asymmetry. It was found in the recent that meridional overturning circulation (MOC) is the most significant source to make the warming difference in both polar regions (e.g., Chylek and others., 2010; Marshall and others., 2014). Here, we will introduce and review these recent findings of MOC to contribute to the asymmetry of warming in the Arctic and Antarctic. This mechanism is in the analogy with the millennial seesaw of temperature found in the paleo ice core records (e.g., Blunier and others., 1998; EPICA community members, 2006), but with a rather short time scale.

2. Twenty century bipolar seesaw of the Arctic and Antarctic surface air temperatures

Cheylek and others. (2010) identified bipolar seesaw patterns in the 20th century the Arctic and Antarctic temperature records for the first time. It is a great surprise that the detrended annual averaged temperatures from meteorological stations north from 64°N and south of 64°S are anti-correlated, as seen in Fig. 1. We could also find a typical "Early 20th century warming pattern" in the Arctic temperature anomaly shown in Fig. 1 top (Yamanouchi, 2011). Cheylec and others. extracted a linear trend (which greenhouse gases

increase must be responsible for) and residual variability (with an 11 year or a 17 year running average), as shown in Fig. 2a. It was found that the residual detrended series were highly anti-correlated, just as the seesaw pattern. The correlation coefficients were r = -0.76 for the 11 year averages and r = -0.89 for the 17 year average. The higher trend of temperature increase in the Antarctic (~2 °C/century) compared to the Arctic (~ 1°C/century) in these hundred years was one point difficult to understand.

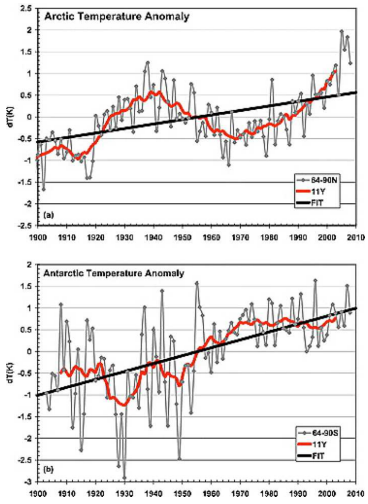

Fig. 1 Temperature anomaly with respect to the 1903-2008 average, its 11 year running mean (red line) and the least square linear fit (thick black line) for the (a) Arctic and (b) Antarctic region. Temperature data used are from the NASA GISS compilation (Chylek and others., 2010).

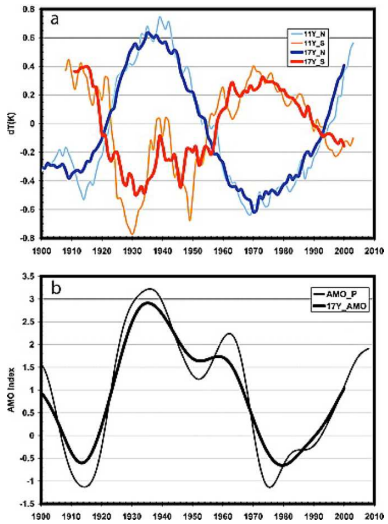

Fig. 2 (a) De-trended Arctic (blue) and Antarctic (red) temperature time series smoothed by a 11 year running average (thin lines) or 17 year running average (thick lines), and (b) the AMO index annual values (thin line) and 17 year running average (thick line) (Chylek and others., 2010).

Cheylec and others. (2010) imagined that the strong anti-correlation of the multidecadal temperature anomalies in the Arctic and Antarctic regions must be due to the ocean, and moreover, the Atlantic Ocean through the high correlation of the residual temperature time series with the Atlantic Multidecadal Oscillation (AMO) index. Knight and others. (2005) explained the AMO to be originated by the variability of the Atlantic Meridional Overturning Circulation (AMOC).

The AMOC is the large scale thermohaline circulation in the world ocean, driven mainly by temperature–salinity buoyancy forces, starts sinking in the North Atlantic, Greenland Sea, and pass through as a deep current through the Southern Ocean (SO) and upwelling in the Pacific. Knight and others., from a 1400 year control run of the coupled climate model, showed that the AMO was strongly related to the variations in the overturning circulation on a near century time scale. Here, a schematic diagram of the overturning circulation called the "Great Ocean Conveyor Belt," published by Wallace Broeker (1987), are shown in Fig. 3, as a popular image that explains the inter-connected ocean circulation and the northward flux of heat in the Atlantic (Richardson, 2008). The AMO index analyzed by Parker and others. (2007) was shown in Fig. 2b. The correlation coefficient with the Arctic temperatures (Fig. 2a) was r = 0.71 for the 11-year AMO index average (r = 0.72 for the 17-year average), while the corresponding anti-correlations with the Antarctic temperature were r = -0.69 (r = -0.80 for the 17-year).

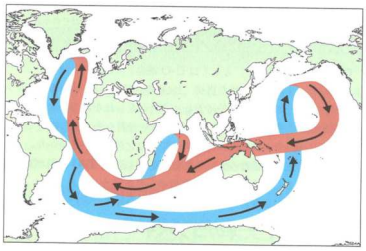

Fig. 3 The great ocean conveyor belt logo shown by Broeker (1987) as illustrated by Joe Le Monier, Natural History Magazine.

3. Asymmetric Arctic and Antarctic responses to greenhouse gas and ozone forcing

We are greatly surprised at the similarity of the sea surface temperature (SST) anomalies distribution by ocean-only model and coupled climate model (15 CMIP5 models) 100 years after an abrupt quadrupling of CO_2 demonstrated by Marshall and others. (2014) in Fig. 4. In both experiments, distinct asymmetries with SSTs in both hemispheres or polar regions were clearly seen. So, the temperature perturbations must be attributable to ocean circulation. It was so striking that this similarity in spatial patterns were mostly a consequence of the underlying ocean circulation rather

than the atmosphere processes under global change. Marshall and others. (2014) discussed these processes using climate response functions (CRFs), the response of the climate to step changes in anthropogenic forcing in which greenhouse gas (GHG) and/or ozone-hole forcing was abruptly turned on.

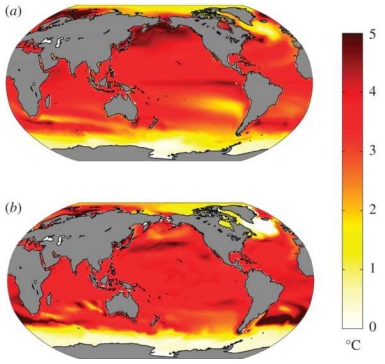

Fig. 4 (a) Ensemble-average SST anomalies 100 years after an abrupt quadrupling of CO_2 in 15 CMIP5 models. (b) SST anomalies after 100 years of an ocean only configuration of the MITgcm induced by a uniform downwelling flux of 4 W m^{-2} and damped at a uniform rate of 1 W m^{-2} K^{-1}, as described (Marshall and others., 2014).

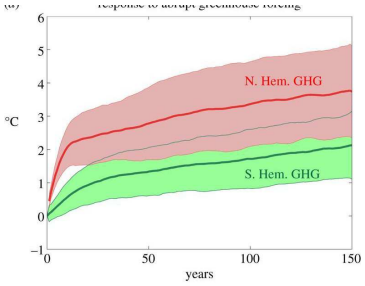

Fig. 5 Sea surface temperature CRFs for GHG forcing computed from an ensemble of 15 CMIP5 models under quadrupling of CO_2. The Arctic is defined as north of 50°N (in red) and the Antarctic between 50°S and 70°S (in green). Thick lines denote the ensemble mean and the shaded area spans 1 s.d. (Marshall and others., 2014)

Fig. 5 shows the response to abrupt GHG forcing. Variations of SST were drawn in the Arctic north of 50°N and the Antarctic between 50° and 70° S under the quadrupling of CO_2. We could find significant differences between the Arctic and the Antarctic. To understand the processes for these responses, heat fluxes and interior temperature structure were examined in Fig. 6. An apparent interhemispheric asymmetry with anthropogenic temperature signal (T_{anthro}) was much larger in the Arctic than in the Antarctic. In Fig. 6a, the time-integrated anomalous air-sea fluxes over hundred years (energy accumulation) is plotted and reveals that most of the energy is fluxed into the ocean around Antarctica due to delayed warming there; however, not stored around Antarctica, but transported to the north and, keeping the Antarctic water cool (Fig. 6b, c). The situation in the Arctic was reversed, and the ocean carried heat into the Arctic, increasing its temperature and then some heat was lost to the atmosphere (Fig. 6a). The advective process was mainly due to the upper cell of the ocean's meridional circulation. This ocean circulation cell, MOC, was a major cause for the interhemispheric asymmetry of the global climate.

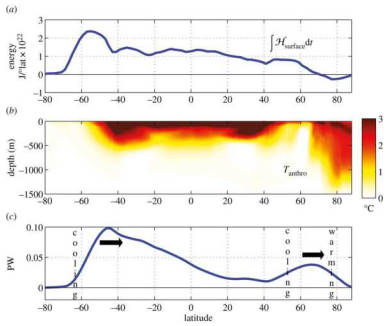

Fig. 6 (a) Surface energy accumulation integrated over 100 years in J/°lat x 10^{22}. (b) Meridional section of zonal-average T_{anthro} after 100 years from the ocean-only configuration of MITgcm whose SST_{anthro} is shown in Fig. 4b. (c) Anomaly in meridional ocean heat transport (in PW) after 100 years relative to control integration. Latitudinal bands of implied ocean warming and cooling are marked (Marshall and others., 2014).

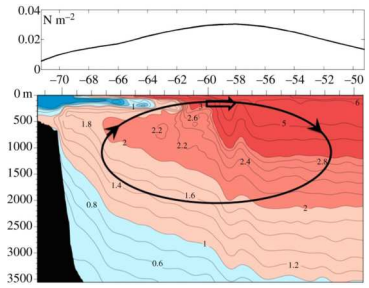

Fig. 7 Meridional hydrographic section of temperature (WOCE section P19) stretching up to Antarctica on the left. The longitude range of the section is 85°-90°W. The region of seasonal sea ice is coincident with cold water (blue tongue) at the surface overlying warmer water (red) below. Superimposed is the sense of the anomalous meridional overturning circulation associated with a positive SAM anomaly, with upwelling around Antarctica and downwelling further equtorward. This acts to warm the ocean just beneath the surface layer. The black line in the top panel shows the SAM-induced zonal wind stress anomaly (Marshall and others., 2014).

The direct effect of ozone-hole forcing on the ocean's surface was due to the surface winds related to Southern Annular Modes (SAM). SST anomaly pattern with cooling around Antarctica and warming

further north was seen firstly. This anomaly could be the direct response of SST to anomalous advection brought by Ekman currents induced by SAM forcing. However, over time, subsurface warming appeared in the top few hundred meters of the ocean and then impacted surface temperatures. So, a cooling came at first, and then came a prolonged warming trend. When the summertime SAM was in its positive phase, upwelling was induced around Antarctica, and downwelling was in further north (Fig. 7). In the upwelling region, a temperature inversion was seen as a consequence of the melting/freezing and export of ice, and resulting freshening of the surface waters appeared. In response to a positive SAM forcing, widespread warming of the ocean was seen just below the mixed layer.

Here, Marshall and others. (2014) clearly explained the mechanism of warming asymmetry in the Arctic and Antarctic derived by ocean circulation, MOC, assumed by Cheylec and others. (2010). The differences in ocean circulation, with sinking in the North Atlantic and upwelling around Antarctica strongly affected the SST response to the GHGs forcing.

4. Delayed warming of Southern Ocean

The SO has shown little warming over the recent decades, in contrast to the rapid warming observed in the Arctic. Armour and others. (2016) presented analyses of oceanographic observations and general circulation model simulations showing fundamentally shaped by the SO's meridional overturning circulation. Fig. 8 showed the observed trends over 1982-2012 when both in situ and satellite observations were available. It was seen that rapid surface warming occurred in zonal bands along the northern side of the Antarctic Circumpolar Current (ACC), and slower warming and cooling appeared to the south. It was clear that these SST patterns were influenced by trends in zonal mean ocean temperature and depth-integrated heat content (Fig. 8c, d). It was found that regions that had warmed strongly had increasingly lost heat to the atmosphere, whereas regions that had warmed less (or cooled) had increasingly taken up the heat. The regions of greatest surface heat uptake showed the least amount of heat storage (Fig. 8b, c). The Southern Hemisphere warming pattern was derived by the meridional ocean heat transport changes. In the south of the ACC, most of the heat taken up had been transported northwards with only a small amount stored locally, and converged along the northern side of ACC. Consequently, it was clearly suggested from observations that the MOC's anomalous heat transport had damped warming south of the ACC and enhanced warming to the north.

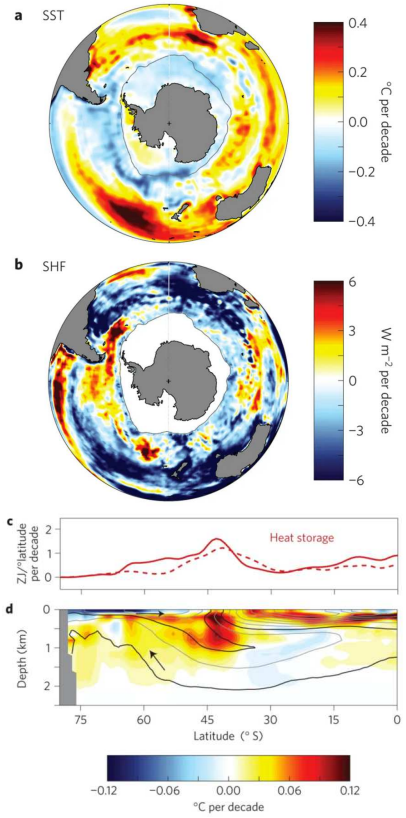

Fig. 8 Observed trends over 1982–2012. **a**, Annual-mean SST trend. **b**, Net SHF trend (positive into ocean). **c**, Zonally and depth-integrated ocean heat content trends from two different subsurface temperature data sets: EN4 (solid; Good and others., 2013) and Ishii (2009; dashed). **d**, Zonal-mean ocean potential temperature trend from EN4, with contours of climatological ocean salinity in intervals of 0.15 practical salinity units (psu) (grey lines). Arrows indicate the orientation of the residual-mean MOC following Karsten and Marshall (2002), along 34.4 and 34.7 psu contours (black lines). Grey line in **a** and **b** shows maximum winter sea-ice extent from Yu and others. (2007) (Armour and others., 2016; Permission for this figure was granted by Springer and Nature).

To quantitatively study the mechanisms driving delayed SO warming, Armour and others. (2016) focused on numerical climate model simulations. The CMIP5 models (GCMs participating in phase 5 of the Coupled Model Intercomparison Project) broadly captured the observed changes over 1982-2012, with little surface warming poleward of the ACC and rapid warming bands along the northern side. Heat storage and warming near the ACC and less warming in the southern side were clearly shown by the models. The 60% of hemispheric surface heat uptake was seen in the region of delayed SO warming, poleward of 50°S, with only 23% of hemispheric heat storage (Fig. 9a). Most of the heat taken up at the surface was transported northwards, by the increase in northward ocean heat transport across the ACC (Fig. 9b), and only a small

portion was stored locally. The heat stored on the equatorward side of the ACC (40° - 50°S) was mainly due to the convergence of heat by the ocean and only less than half from local surface heat uptake. These model results were mostly consistent with the observations (Fig. 8). Delayed SO warming, which was driven by anomalous northward ocean heat transport, seemed to be a fundamental ocean response to GHG forcing. The observed cooling of the SO as seen in Fig. 8a was not explained enough; however, the delayed SO and its driving mechanisms were clarified against a background GHG-induced warming, compared to the rapid warming in the Arctic.

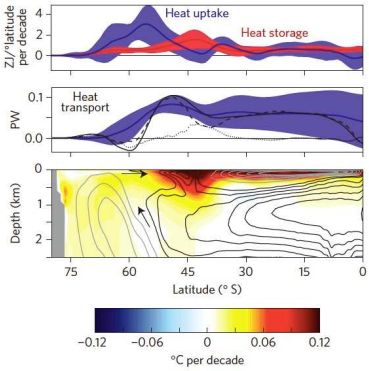

Fig. 9 CMIP5-mean trends over 1982–201. **A**, Zonally integrated average SHF (blue) and full-depth ocean heat content trend (red). **B**, Anomalous OHT for CMIP5-mean (blue) and CCSM4 (black; solid, dashed and dotted lines show total, residual-mean advection and diffusion, respectively). **C**, Zonal-mean ocean potential temperature trend, with contours showing the MOC from CCSM4 (black contours show positive circulation in 4 Sv increments, grey contours show negative circulation in 4 Sv increments) (Armour and others.,2016; Permission for this figure was granted by Springer and Nature).

Now, Armour and others. (2016) verified the mechanism of MOC within the SO from observations and CMIP5 modeling to enhance heat transport to the north and bring the SAT or SST variations, especially in the SO, which Marshall and others. (2014) outlined by the model results.

5. Recent recognitions of MOC

We have followed the role of MOC to enhance north-south asymmetry in the climate, then, what is the actual condition of MOC. There was already long history of discussions of MOC. Richardson (2008) had shown the discussion based on the history of MOC schematic diagrams before and after Blocker's simple schematics (Fig. 3). Lozier (2010) pointed out the over simplified image of ocean conveyor-belt (Fig. 3), and indicated the importance of wind and eddy field as the forcing. Marshall and Speer (2012) presented a reconsideration of MOC, focusing to the SO. They presented the importance of the SO upwelling branch of the MOC circulation together with a "two-cell MOC," one was a southward deep flow counter back to northward shallow flow, and another was a southward deep flow with counter back as deep water.

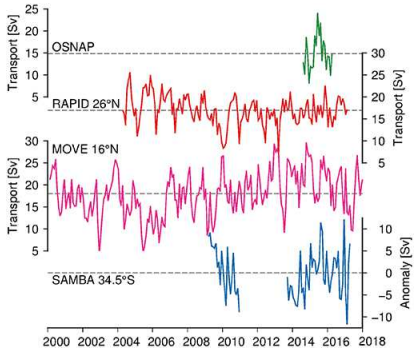

Fig. 10 Monthly values of *MOCz* transport from four observing arrays: OSNAP (green), RAPID 26◦N (red), MOVE 16◦N (magenta) and SAMBA 34.5◦S (blue). For SAMBA, the transports are shown as anomalies. The respective means are given by the black dashed line (zero in the case of SAMBA) (Frajka-Williams, E. and others., 2019).

Actual observations of transport and variability of MOC are limited only to the recent activities. Frajka-Williams and others. (2019), based on the meridional cross section of salinity and ocean circulation originally drawn by Lozier (2012) just as similar to the two cell MOC by Marshall and Speer (2012), presented many observational amounts of MOC transport. Even though a long data set showed a decline in AMOC, this data set was assumed to be biased due to the seasonal variability of single hydrographic measurements at each timing. Continuous measurements have been made already by six active observing arrays in the Atlantic. One cross-section, OSNAP (Overturning in the Subpolar North Atlantic Program), was launched to provide an observational basis for a slowing AMOC in the 21st century (Lozier and others., 2019). From their 21-month records, no clear trend could be derived. Frajka-Williams and others. (2019) showed four records including OSNAP as Fig. 10, but still the long record was limited, and a long term trend was not clear but records were fairly stable. The mean strength of AMOC was about 15 to 18 Sv (10^6 m^3/s). So, from these results, inter decadal variability as proposed by Cheylec and others. (2010) shown in Fig. 1 could not be confirmed simply by the data of MOC yet. We need to obtain these observational data for a long duration.

6. Conclusion

We have reviewed the progress of studies in the recent decade of how MOC contributes to the large

North-South asymmetry in warming. The variation of MOC could clearly explain multidecadal SAT variations in the Arctic and Antarctic. MOC strongly influenced the sea surface temperature response to anthropogenic GHG forcing, accelerating warming in the Arctic while delaying it in the Antarctic. Anomalous transport of heat by the MOC was shown to damp warming in the SO and enhance warming to the north. MOC was an effective source to make the warming difference in both polar regions; however, the contributing ratio compared to the other agent is a future subject. In the 1990s and 2000s, AMOC was observed as about 15 to 18 Sv (Frajka-Williams and others., 2019); however, no direct comparison in multidecadal time scale with damping effect was made yet.

References

Armour, K. C., Marshall, J., Scott, J. R., Donohoe, A. and Newsom, E. R. (2016): Southern Ocean warming delayed by circumpolar upwelling and equatorward transport. *Nature Geo.*, **9**, 549-554. http://dx.doi.org/10.1038/ngeo2731.

Blunier, T. and 11 others (1998): Asynchrony of Antarctic and Greenland climate change during the last glacial period. *Nature*, **394,** 739-743, doi: 10.1038/29447.

Broecker, W.S. (1987): The biggest chill. *Natural History Magazine,* **97**, 74–82.

Cheylek, P., Folland, C. K., Lesins, G. and Dubey, M. K. (2010): Twentieth century bipolar seesaw of the Arctic and Antarctic surface air temperatures. *Geophys. Res. Lett*., **37**, L80703. doi:10.1029/2010GL042793.

EPICA community members (2006): One-to-one coupling of glacial climate variability in Greenland and Antarctica. *Nature*, **449**, 195-198, doi:10.1038/nature05301.

Frajka-Williams, E. and 40 others (2019): Atlantic meridional overturning circulation: observed transport and variability. *Frontiers Marine Sci.*, **6**, 260, doi: 10.3389/fmats.2019.00260.

Good, S. A., Martin, M. J. and Rayner, N. A. (2013): EN4: quality controlled ocean temperature and salinity profiles and monthly objective analyses with uncertainty estimates. *J. Geophys. Res.,* **118,** 6704_6716.

Goose, H. and 13 others (2018): Quantifying climate feedback in polar regions. *Nature Comm.*, DOI: 10.1038/s41467-018-04173-0.

Hansen, J., Sato, M., Kharecha, P. and von Schuckmann, K. (2011): Earth's energy imbalance and implications. *Atmos. Chem. Phys.,* **11**, 13 421–13 449. doi:10.5194/acp-11-13421-2011.

Ishii, M. and Kimoto, M. (2009): Reevaluation of historical ocean heat content variations with time-varying XBT and MBT depth bias corrections. *J. Oceanogr.* **65,** 287_299.

Karsten, R. H. and Marshall, J. (2002): Constructing the residual circulation of the ACC from observations. *J. Phys. Oceanogr.*, **32,** 3315_3327.

Knight, J. R., R. J. Allan, C. K. Folland, M. Vellinga, and M. Mann (2005): A signature of the persistence natural thermohaline circulation cycle in observed climate. *Geophys. Res. Lett.,* **32**, L20708, doi:10.1029/2005GL024233.

Lozier, M. S. (2010): Deconstructing the conveyer belt. *Science*, **328**, 1507-1511.

Lozier, M. S. (2012): Overturning in the North Atlantic. *Ann. Rev. Mar. Sci*. **4**, 291–315. doi: 10.1146/annurev-marine -120710-100740.

Lozier, M. S. and 37 others (2019): A sea change in our view of overturning in the subpolar North Atlantic. *Science,* **363**, 516-521,

Marshall, J. and Speer, K. (2012): Closure of the meridional overturning circulation through Southern Ocean upwelling. *Nature Geosci.* **5,** 171_180.

Marshall, J., Armour, K. C., Scott, J. R., Kostov, Y., Hausmann, U., Ferreira, D., Shepherd, T. G. and Bitz, C. M. (2014): The ocean's role in polar climate change: asymmetric Arctic and Antarctic responses to greenhouse gas and ozone forcing. *Phil. Trans. R. Soc.* **A 372**, 20130040. hdoi.org/10.1098/rsta.2013.0040.

Parker, D. E. and 7 others (2007): Decadal to interdecadal climate variability and predictability and the background of climate change, *J. Geophys. Res.*, **112**, D18115, doi:10.1029/2007JD008411.

Richardson, P. L. (2008): On the history of meridional overturning circulation schematic diagrams. *Prog. Oceanography*, **76**, 466-486. doi:10.1016/j.pocean.2008.01.005.

Salzmann, M. (2017): The polar amplification asymmetry: role of Antarctic surface height. *Eath Syst. Dynam*., **8**, 323-336, doi:10.5194/esd-8-323-2017.

Thompson, D.W.J. and Solomon, S. (2002): Interpretation of recent Southern Hemisphere climate change. *Science*, **265**, 895-899, doi:10.1126/science.1069270

Yamanouchi, T. (2011): Early 20th century warming in the Arctic: A review. *Polar Science*, **5**, 53-71, doi:10.1016/j.polar.2010.10.002.

Yamanouchi, T. (2019): Arctic warming by cloud radiation enhanced by moist air intrusion observed at Ny-Ålesund, Svalbard. *Polar Science*, **21**, 110-116, doi.org/10.1016/j.polar.2018.10.009.

Yu, L. and Weller, R. A. (2007): Objectively analyzed air-sea heat fluxes for the global ice-free oceans (1981_2005). *Bull. Am. Meteorol. Soc.* **88,** 527_539.

Summary in Japanese

和文要約

北極温暖化増幅と東南極温暖化抑制
－ 子午面逆転循環（MOC）の南北非対称への寄与 －

山内　恭[1,2]

[1]国立極地研究所、[2]総合研究大学院大学極域科学専攻

北極では温暖化増幅が、南極では温暖化抑制が見られる。地球温暖化の下でこの大きなコントラストをもたらすものは何だろうか？ このコントラストをもたらすいくつかのメカニズムについては既に議論されているが、最も効果的なものの 1 つが、海洋循環、特に子午面逆転循環（MOC）と呼ばれるものだろう。ここでは、MOC が温暖化における南北の大きな非対称性をどのようにもたらしているかについて、過去 10 年間の研究の進捗をレビューした。

Correspondence to: T. Yamanouchi, yamanou@nipr.ac.jp